Taylor & Francis
Taylor & Francis Group

RESEARCH ARTICLE

OPEN ACCESS | Check for updates

Sorafenib-associated translation reprogramming in hepatocellular carcinoma cells

Laura Contreras [a,b]*, Alfonso Rodríguez-Gil [a,c]*, Jordi Muntané [a,c,d], and Jesús de la Cruz [a,b]

aInstituto de Biomedicina de Sevilla, Hospital Universitario Virgen del Rocío/CSIC/Universidad de Sevilla, Seville, Spain; bDepartamento de Genética, Facultad de Biología, Universidad de Sevilla, Seville, Spain; cDepartamento de Fisiología Médica y Biofísica, Universidad de Sevilla, Seville, Spain; dCentro de Investigación Biomédica en Red de Enfermedades Hepáticas y Digestivas (CIBEREHD), Instituto de Salud Carlos III, Madrid, Spain

ABSTRACT

Sorafenib (Sfb) is a multikinase inhibitor regularly used for the management of patients with advanced hepatocellular carcinoma (HCC) that has been shown to increase very modestly life expectancy. We have shown that Sfb inhibits protein synthesis at the level of initiation in cancer cells. However, the global snapshot of mRNA translation following Sorafenib-treatment has not been explored so far. In this study, we performed a genome-wide polysome profiling analysis in Sfb-treated HCC cells and demonstrated that, despite global translation repression, a set of different genes remain efficiently translated or are even translationally induced. We reveal that, in response to Sfb inhibition, translation is tuned, which strongly correlates with the presence of established mRNA cis-acting elements and the corresponding protein factors that recognize them, including DAP5 and ARE-binding proteins. At the level of biological processes, Sfb leads to the translational down-regulation of key cellular activities, such as those related to the mitochondrial metabolism and the collagen synthesis, and the translational up-regulation of pathways associated with the adaptation and survival of cells in response to the Sfb-induced stress. Our findings indicate that Sfb induces an adaptive reprogramming of translation and provides valuable information that can facilitate the analysis of other drugs for the development of novel combined treatment strategies based on Sfb therapy.

Introduction

Hepatocellular carcinoma (HCC) is one of the most lethal and fastest-growing tumours worldwide, with a poor prognosis in both men and women [1]. The occurrence and development of HCC is a complex issue involving a mixture of different aetiologies, including chronic hepatitis B and C, metabolic-associated fatty liver disease (MAFLD), alcohol abuse, aflatox-ins-containing nutrients, and smoking [2].

As occurring with many other cancers, the prognosis and treatment of HCC vary depending on the staging of the tumour and the hepatic function of the patients [3]. While curative treatments such as local ablation, surgical resection and orthotopic liver transplantation are indicated at very early stages of the disease, chemoembolization is recommended for the intermediate stages, as well as the systemic therapy is recommended for the advanced stages of the disease [3]. Immunotherapy (e.g. Atezolizumab *plus* Bevacizumab, Durvalumab and Tremelimumab) has implied significant improvement of the survival of patients with advanced HCC patients [4]. However, in many cases, immunotherapy is not feasible or has no beneficial effect compared to classical treatments in patients without preserved liver function, high risk for bleeding, vascular disorders, arterial hypertension, severe

autoimmune disorders, or immunosuppression and MALFD [3]. Non-alcoholic fatty liver disease (NASH), which is the most severe form of MAFLD, limits anti-tumour surveillance in immunotherapy-treated HCC [5]. Thus, tyrosine kinase inhibitors (TKIs), including Sorafenib (Sfb), Lenvatinib and Regorafenib, provide the only first- or second-line therapeutic option for a significant number of HCC patients in the advanced stage of the disease [6]. Unfortunately, TKIs only provide very limited clinical benefits as consequence of widely developed resistance, making it imperative to develop novel and more effective therapeutic combinations to improve the outcome of patients with advanced-stage HCC [7,8].

Sfb exerts a potent antiproliferative and pro-apoptotic activity against HCC cells [9]. The activity of the drug is associated with an early but gradual increase of endoplasmic reticulum (ER) stress, which leads to the induction of apop-tosis [10,11]. We and others have shown that Sfb strongly inhibits the initiation step of protein synthesis [11,12]. However, how Sfb causes this inhibition has not yet been completely elucidated. Moreover, the overall changes in mRNA translation that occur in HCC cells after an Sfb-treatment have neither been explored. The aim of the present study was to examine the landscape of translation in liver

---

cancer cells in response to a therapeutic concentration of Sfb. To do this, we performed a genome-wide polysome profiling analysis coupled with Next-Generation Sequencing (NGS) in HepG2 cells, before or after an Sfb-treatment, to identify those mRNAs that are differentially translated under these conditions as a resource for the future development of novel therapeutic strategies.

Materials and methods

Cell lines, culture conditions and treatments

The HepG2 cell lines were obtained from the American Type Culture Collection (LGC Standards, Barcelona, Spain). The Huh7 cell line was purchased from Apath, LLC (Brooklyn, NY, USA). Both cell lines tested negative for mycoplasma contamination. Cells were cultured in minimal essential medium (MEM) with Earle's balanced salts with L-glutamine (ref. E15–825, PAA Laboratories Inc., Toronto, Canada) supplemented with 10% foetal bovine serum (FBS, ref. F7524, Sigma Aldrich, St. Louis, MO, USA), 1% sodium pyruvate (ref. S11–003, PAA Laboratories Inc.), 1% non-essential amino acids (ref. M11–003, PAA Laboratories Inc.) and penicillin–streptomycin solution (100 U/ml-100 µg/ml; ref. P11–010, PAA Laboratories Inc.).

Cells were grown as previously described [13]. Briefly, cells were cultivated in flasks at 37°C in a humidified incubator with 5% CO_2 until reaching a density of 100,000 cells/cm^2. Sorafenib (Sfb, Sorafenib tosylate, ref. FS10808; Carbosynth Ltd., Compton, UK) was dissolved in dimethyl sulphoxide (DMSO) as a stock solution (100 mm), aliquoted, and stored at −80°C. For drug treatment, cells were cultivated for 24 h; then, Sfb was added at a concentration of 10 µM, and lysates were obtained after a 12 h treatment. Control cells were treated with the vehicle DMSO. Sfb was used at the concentration of 10 µM, as this concentration is very similar to that reported in the plasma of patients after a Sfb standard administration [14].

Polysome profiling and fractionation

Polysome profile analysis was carried out in Sfb-treated and control HepG2 cells as previously described [11]. Briefly, cells were produced to ca. 70% confluency in 100 mm dishes as above described. Normally, two dishes were used per condition assayed. Before harvesting, 200 µg/ml cycloheximide (ref. C7698, Sigma Aldrich) was added to dishes and incubated for 5 min at 37°C. Each dish was then placed on ice, the media aspirated and the cultures washed twice with PBS without Ca^{2+} and Mg^{2+} containing 200 µg/ml cycloheximide. Then, 600 µl of lysis buffer (10 mm Tris-HCl, pH 7.4, 150 mm NaCl, 10 mm $MgCl_2$, 200 µg/ml cycloheximide, 2 mm DTT, 0.5% NP40) was added to one dish, cells were scraped and transferred to the second dish. After scraping the cells corresponding to the second dish, they were transferred to a 1.5 ml-Eppendorf tube. Tubes were incubated at 4°C with gentle end-over-end rotation for 10 min and then centrifuged at 16,000 x g for 8 min at 4°C in a refrigerated microfuge. The corresponding supernatants were recovered and the A_{260} measured

using a NanoDrop ND-1000 Spectrophotometer (Thermo Fisher Scientific, Waltham, MA, USA). About 11 A_{260} units were layered on top of 10–50% (w/v) sucrose gradients prepared in a buffer containing 50 mm Tris-acetate, pH 7.5, 50 mm NH_4Cl, 12 mm $MgCl_2$, and 1 mm DTT. The gradients were centrifuged at 260,110 × g (39,000 rpm) in a Beckman SW41Ti rotor at 4°C for 2 h 45 min. Fractionation was performed with an ISCO UA-6 system (Teledyne ISCO, Lincoln, NE, USA) equipped to continuously monitor the A_{254}.

When required, fractions of 1 ml were collected from the gradients. Fractions corresponding to the low-molecular complex peak and the peaks corresponding to free 40S and 60S ribosomal subunits and 80S ribosomes were pooled and named 'low-translated fraction' or V1. Fractions corresponding to the polysome peaks were pooled and named 'high-translated fraction' or V2.

mRNA library preparation

Libraries were prepared using the RNA collected from the V1 and V2 fractions described above. Samples were treated with a proteinase K solution (per 1 ml: 37.5 µl 10% SDS, 7.5 µl 0.5 M EDTA, and 4 µl 20 mg/ml proteinase K, ref. A7932, Sigma Aldrich) for 1 h at 50°C. An equal volume of phenol acidic: choroform:isoamyl alcohol (25:24:1, v/v) was added to the sucrose fractions; samples were mixed during 30 s using a vortex and centrifuge 10 min at maximum speed at 4°C. Approximately 80% of the aqueous phase was placed in a new tube, and an equal volume of chloroform was added. After mixing for 30 s using a vortex, the samples were centrifuged 10 min at maximum speed at 4°C. Again, 80% of the aqueous phase was placed in a new tube, and the RNA was precipitated using 1:10 of 3 M sodium acetate, pH 5.2 and 1.5 volumes of absolute ethanol. The mixture was incubated overnight at −20°C. Samples were then centrifuged at maximum speed for 30 min at 4°C, the pellet was washed with 70% ethanol and finally resuspended in RNase-free water.

The concentration and quality of RNAs were assessed with Qubit (Qubit^{TM} DNA HS assay, Thermo Fisher Scientific) and a 2100 Bioanalyzed Nano Chip (Agilent Technologies Genomics, Santa Clara, CA, USA), respectively. The RNA Integrity Number (RIN) values were >9 in all the RNA samples. Polyadenylated RNA was isolated from total RNA samples using NEBNext Oligo d(T)$_{25}$ beads (New England Biolabs, Ipswich, MA, USA) according to the manufacturer's instructions. The same RNA concentration for each sample was used to create the libraries for Illumina Sequencing. Three independent experiments were carried out for the sequencing analysis.

RNA sequencing and data analyses

RNA sequencing was performed with a NextSeq500 Mid-Output and 2 × 75pb length parameters (paired-end). RNA-Seq data were first filtered using the FASTQ Toolkit v1.0.0 program and then analysed using the BaseSpace Onsite v3.22.91.158 from Illumina. Only genes that were upregulated or downregulated with a p-value <0.05 and [log$_2$(fold change)] ≥ ± 0.5 were selected. Data were normalized using

the z-score. The $\log_{10}(V2/V1)$ was applied to calculate the translation level (TL) for each gene in both the control and Sfb-treated conditions. A positive TL reflects a higher proportion of mRNA in V2 than the average. A negative value corresponds to those mRNAs with an enrichment in V1. Applying this criterion, we identified two sets of genes for each condition: (i) a set enriched in mRNAs with a positive TL and (ii) a set enriched in mRNAs with a negative TL.

The previous data were combined to identify the changes in the translational behaviour of mRNAs in response to the Sfb treatment. Four additional categories were identified (i) a gene set enriched in mRNAs with a positive translation ratio in both conditions, (ii) a gene set enriched in mRNAs with a negative translation ratio in both conditions, (iii) a gene set enriched in mRNAs with a positive ratio in Sfb-treated and a negative ratio in untreated cells and (iv) a gene set enriched in genes with a negative ratio in Sfb-treated and positive in untreated cells.

Data from the sequencing reads were deposited in Gene Expression Omnibus (GEO; https://www.ncbi.nlm.nih.gov/geo/) under the accession number GSE282706.

Over-representation analysis (ORA)

To identify the mRNA features present in the different categories described above, an Over-Representation Analysis (ORA) was performed using a Fisher's exact test, selecting the genes with a p-value lower than 0.05 in the RNA-Seq data, either in each condition or in both conditions simultaneously. Different databases were used for the enrichment analysis [15–22]. A REACTOME database (https://reactome.org) was used to investigate either activated or inhibited pathways of the differentially expressed genes in both control and Sfb-treated cells.

Real-time quantitative PCR

To validate the results of the RNA-Seq analysis, the relative RNA abundance of randomly selected mRNAs was quantified by real-time quantitative PCR (RT-qPCR). After polysome fractionation, 100 µl of each fraction was taken from the sample representing the total RNA content in the profile. Then, the rest of each fraction was pooled together in V1 and V2 samples and before RNA extraction, 0.5 µg of a commercial luciferase RNA control (cat. L4561, Promega, Madison, WI, USA) in a volume of 2 µl was added to each one. Note that, in addition to using pooled samples, specific mRNAs were also analysed along all the profile so the polysome fractions were individually handled. Then, RNA was extracted as described above and equal volumes of RNA samples were treated with 1 µl of DNase I (ref. Z3585, Promega) following the manufacturer's instructions. RNA was then reverse transcribed using SuperScript^{TM} III First Strand Synthesis for RT-PCR, also according to the manufacturer's instruction (ref. 18080051, Invitrogen, Thermo Fisher Scientific) using random hexamer primers (ref. N8080127, Hoffman-La Roche, Basel, Switzerland). RT-qPCR was performed using SYBR® Green Premix Ex Taq^{TM} 2X (ref. RR390A, Takara Bio Inc., Kusatsu, Japan) and specific primers for each transcript. The results were normalized to the total whole profile RNA. The luciferase RNA, added to each sample before the RNA extraction, was used as an additional control for the extraction efficiency. The percentage of mRNA was calculated, and the data were expressed as the mean ± standard deviation of the mean.

The primer sequences are:

For eIF4E2:
5'TGAAAGATGATGACAGTGGGGA 3' (forward)
5'CTGATTCTTGTCTCGTTCCGT 3' (reverse)

For ERBB2:
5'CTACTCGCTGACCCTGCAAG 3' (forward)
5'TGTTATGGTGGATGAGGGCC 3' (reverse)

For CSK:
5'CCAACTACCCCGGAGACTAC 3' (forward)
5'AGTACACCTCCTCGTCGATG 3' (reverse)

For RAD51:
5'GCACTGGAACTTCTTGAGCA 3' (forward)
5'GTTGTTTTCATTAAGGGCACTCC 3' (reverse)

For NDUFA7:
5'AACTCAGCCTCCTCCCAAG 3' (forward)
5'CTCTCTGCTGGCTTGCCT 3' (reverse)

For SMAD7:
5'CCCCTCCTCTCCCTCATCAA 3' (forward)
5'GGCTGGCAGGAAGGGAATAA 3' (reverse)

For CPEB4:
5'CACCAACACCCTCCTCCTCC 3' (forward)
5'TTCAGGGGCGTTATTCCACC 3' (reverse)

For PCNA:
5'AAAGTCCAAAGTCAGATCTGGTC 3' (forward)
5'ACTGCATTTAGAGTCAAGACCCT 3' (reverse)

For Luciferase gene:
5'ATCCGGAAGCGACCAACGGG 3' (forward)
5'GTCGGGAAGACCTGCCACGC 3' (reverse)

Statistical analysis

For RNA-Seq, three biological replicates were obtained. Data from validations were generated from several repeats (at least three) of different biological replicates (at least three). The mean ± standard error of the mean data were represented in the different graphs. To determine significance, the Student's t-test for unpaired samples with confidence interval of 95% was computed. Statistical analyses were performed with the Prism 6.01 software (Insight Partners, NY, USA). Significance between conditions was indicated with the symbols $*p < 0.05$, $**p < 0.01$, $***p < 0.001$, and $****p < 0.0001$. Regression plots and determination of Pearson coefficients and p-values were performed using the R software.

Results and discussion

Cancer cells modify protein synthesis, which impacts the selective translation control of specific subsets of mRNAs, allowing them to proliferate, migrate, and survive in adverse conditions. Thus, translation has been strongly linked to chemotherapy response and resistance [23,24]. Translation is a crucial process in hepatocytes, which secretome is particularly relevant in the context of physiopathology [25]. Sfb

remains a relevant treatment in HCC. It is known that translation is a key target of Sfb. Thus, Sfb has been shown to inhibit translation at the initiation level as well as affect the mTOR signalling pathway, activate PERK and induces the formation of stress granules in HCC cells [11,12,26]. To better understand the mode of action of Sfb and its consequences on translation and identify how this drug exerts an overall change in the translational status of HCC cells, we performed a genome-wide polysome profiling approach. We firmly believe that this analysis could not only clearly help understanding the mechanism of action of Sfb but also the reasons for its modest effectiveness in HCC patients. We focused on the human hepatoblastoma cell line, HepG2, which has been extensively used for investigating a wide range of studies related with the oncogenesis or the cytotoxicity of different substances, including Sorafenib, on the liver [27].

With this aim, extracts from HepG2 cells untreated or treated with 10 μM Sfb for 12 h were subjected to polysome profile analysis. Fractions were differentially collected into two pools, the V1 fraction, corresponding to free mRNAs or mRNAs bound to monosomes, and the V2 fraction, corresponding to mRNAs with two or more engaged ribosomes. Total RNA was extracted from the pools, and mRNA was purified using oligo (dT) paramagnetic beads and subjected to Illumina RNA sequencing. Three independent biological replicas were obtained, and the total counts were calculated for each gene (Supplementary Figure S1). The appropriately normalized data were used to estimate the translation level (TL) of the genes by calculating the logarithm of V2/V1. Z-scores of Sfb-treated and untreated samples were also calculated to reveal gene-specific changes over the general

translation inhibition exerted by Sfb. We established that those mRNAs with a negative TL represent poorly translated mRNAs, while those with a positive TL correspond to actively translated mRNAs (Figure 1A). Then, we compared the TL obtained for untreated and Sfb-treated cells to establish how gene-specific translation changes after the treatment. Applying this approach, we were able to define eight populations of genes (Figure 1B), including those whose translation is selectively enhanced or inhibited upon the Sfb treatment. All data were organized into a Microsoft Excel sheet to manually identify the different parameters of the genes in our analysis, included the TL, by just typing the gene name (see Supplementary Dataset S1). To validate the results, we performed polysome profile analysis of control-untreated and Sfb-treated cells and collected fractions. Then, different genes were randomly selected, including eIF4E2, ERBB2, CSK, RAD51, NDUFA7 and SMAD7, and the association of their corresponding mRNAs with the translationally active pool of ribosomes tested by RT-qPCR in the fractions. Results of the different RT-qPCRs were consistent with the TL values obtained after RNA sequencing, indicating that the genome-wide analysis provided reliable data (Supplementary Figures S2A and S2B). To ensure that the obtained results were not specific to the particular HepG2 cell line, different genes were selected for RT-qPCR in cells of the HCC Huh7 cell line, including SMAD7, RAD51, PCNA, CPEB4 ERBB2 and CSK, whose distribution in polysomes was also tested. Results are shown in Supplementary Figure S3.

Next, we aimed to define the mechanisms underlying the different translation behaviours of genes in response to the Sfb-treatment. To this end, we performed an over-
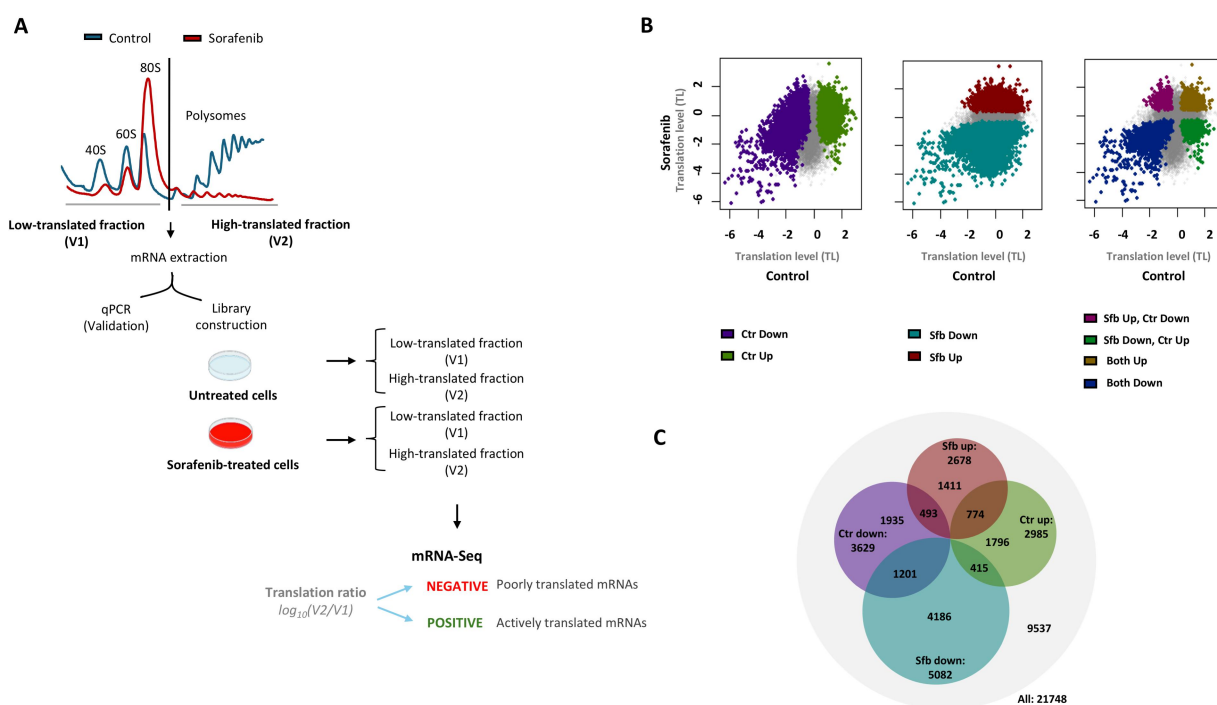

Figure 1. Ribo-Seq analysis of untreated and Sfb-treated HCC cells. A. Scheme of the workflow for the polysome profile analysis and calculation of the translation level (TL) parameter. B. Dot plots showing the TL of control or untreated (X-axis) and Sfb-treated samples (Y-axis). Genes whose translation is significantly influenced in a positive or a negative manner in each single or in combinations condition are highlighted. C. Proportional Venn diagram showing the number of genes whose translation is positively or negatively influenced in each condition (p- value < 0.05; TL < − 0.5 or > 0.5).

representation analysis (ORA) to identify specific mRNAs features that could be involved in the Sfb-mediated translation regulation of the genes from the above eight defined categories. Consistent with the general translation initiation inhibition exerted by Sfb [11,12], we found that the number of significant poorly translated mRNAs in Sfb-treated cells was higher than the number of poorly translated mRNAs in control cells even after an intra-sample normalization (Figure 1C). Moreover, we also found that the changes in the TL parameter, both in the control and Sfb-treated conditions, showed no correlation with the changes in total mRNA levels upon Sfb treatment (Supplementary Figure S4). These data were obtained by high-throughput RNA-Seq technology and were separately reported [13]. Thus, our results suggest that the translation reprogramming induced by Sfb is independent of other gene regulation processes, such as mRNA transcription or mRNA stability, which Sfb could also be modifying.

We reveal that translation is tuned by established mRNA *cis*-acting elements upon the Sfb treatment:

(i) As Sfb induces ER stress characterized by an increase in the phosphorylation levels of eIF2α at serine 51 under activation of PERK (e.g. [10,11]), there was a significant enrichment of mRNAs with upstream open reading frames (uORFs) in their 5' untranslated regions (5' UTRs) within the category with a positive TL in Sfb-treated cells (p-value 5.54×10^{-60}; Supplementary Dataset S2). Among them, the gene for the transcription factor ATF4 and many of its targets including DDIT3, GADD34, STC2 and ATF3; many of these proteins are produced to mitigate a wide range of stresses (i.e. hypoxia, nutrient deprivation, ER and oxidative stress) or induce cell death if the stress is not resolved [28]. Other genes with a positive TL upon the Sfb-treatment were those coding for NOL6, NCL, EIF4G1, FTSJ3 and KRI1, which are all factors involved in ribosome biogenesis; this process has been reported to promote proliferation, migration, and invasion in cancer cells of different tumours (e.g. [29–31]). We speculate that this up-regulation reflects the activation of a feedback response to mRNA translation inhibition. Indeed, it has been reported that, in case of dysfunctional mRNA translation, to restore ribosome homoeostasis, there is activation of a particular signalling pathway that stimulates the transcription of c-Myc to induce ribosome biogenesis [32].

(ii) Cytoplasmic polyadenylation element-binding protein 4 (CPEB4) is also encoded by an uORF-containing gene; thus, its induction is also subjected to regulation by eIF2α phosphorylation [33]. CPEB4 binds mRNAs containing CPEs in their 3' UTR to maintain the translation of these mRNAs in conditions in which global protein synthesis is inhibited [33]. As a result, and although CPEB4 itself was not found to be significantly up-regulated by the Sfb-treatment, several CPEB4 target genes were enriched in the set of genes translationally up-regulated by Sfb (p-value 1.52×10^{-8}; Supplementary Dataset S3).

(iii) More importantly, mRNAs containing AU-rich elements (AREs) in their 3' UTRs were significantly enriched in the set of genes translationally up-regulated by Sfb, but poorly represented in the remaining categories (p-value 4.54×10^{-54}; Supplementary Dataset S4). Although, the relevance of this observation is still unclear, it clearly suggests that AREs and specific ARE-binding proteins may play important roles in the translation reprogramming caused by the Sfb treatment.

(iv) Moreover, we and others have shown that Sfb negatively affects canonical cap-dependent translation ([12], L.C., in preparation); however, cells encompass several alternative modes of translation initiation that bypass the cap binding of eIF4F, including that supported by DAP5, also known as EIF4G2 [22,34]. We then examined how DAP5-target genes respond to the Sfb treatment. As a result, we identified that DAP5-target genes were also significantly enriched in the set of genes up-regulated by Sfb (p-value 3.71×10^{-30}; Supplementary Dataset S5). A deeper observation intriguingly showed that DAP5-target mRNAs with a high positive TL in the Sfb-treated samples have a low negative TL in the control cells. In turn, other distinct DAP5-target genes were enriched in those mRNAs with a positive TL in control conditions, which, surprisingly, showed a negative TL upon the Sfb treatment. Indeed, when we pooled all genes with this particular behaviour from our datasets, which we named the 'family of genes with opposite direction' (genes with positive TL in control conditions but negative TL in Sfb-treated cells and genes with negative TL in control conditions but positive TL in Sfb-treated cells), we found that this family was significantly enriched in DAP5-target genes (p-value 7.00×10^{-41}; Supplementary Dataset S6 and Supplementary Dataset S7). Further experiments are required to understand this relevant feature of DAP5-mediated translation upon the stress induced by Sfb in HCC cells.

(v) Because DAP5 also participates in several cap-independent modes of translation initiation, including those using internal ribosome entry sites or IRESs (e.g. [35]), we also checked the distribution of IRES-containing mRNAs in our different datasets. As a result, we found that IRES-containing mRNAs showed a tendency similar to that observed for DAP5-target genes, thus, also belonging to the 'family of genes with opposite direction'. In this case, the p-value was much lower (p-value 9.97×10^{-6}; Supplementary Dataset S8). All these findings are summarized in Figure 2.

Regarding genes whose translation is negatively influenced by Sfb, we highlighted a strong correlation between the TL of the genes and the length of their respective coding regions (CDS). Thus, the CDS of those genes with a high positive TL
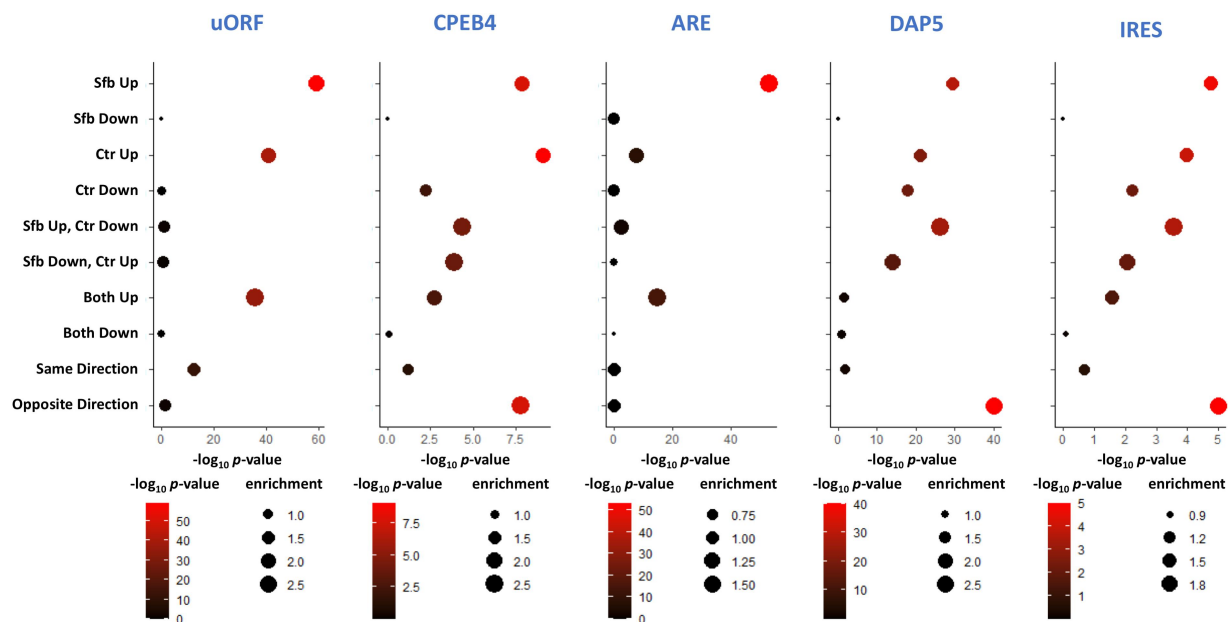
Figure 2. Functional enrichment analysis. Bubble plots depicting the over-representation analysis (ORA) of different mRNA features or *cis*-acting elements (from left to right, uORF containing mRnas, CPEB4 target mRnas, are-containing mRNAs in their 3' UTRs, DAP5 target mRNAs and IRES containing mRNAs) in the gene categories defined in Figure 1B. In each plot, the -log$_{10}$ (*p*-value) of the ORA is shown in the X-axis. A colour scale is applied. The size of each bubble corresponds to the enrichment of each feature as the number of genes with the studied feature in each category *versus* the total number of genes with the feature and normalized by the number of genes in the group *versus* the total number of genes represented in the RNA-Seq file.

in the control condition samples were normally shorter than average, while that of genes with a high positive TL in Sfb-treated cells was longer than average, suggesting that mRNAs with a long CDS are more resistant to the translation inhibitory effect of Sfb. These tendencies were even more evident in the sets of genes actively translated in one condition (control-untreated or Sfb-treated conditions) and poorly translated in the other (Supplementary Figure S3). Still, the genes whose translation was clearly more affected by Sfb (those that we designated 'Sfb hypersensitive genes') did not follow such a tendency. Indeed, two clear populations could be observed when plotting the TL *versus* the CDS length in the Sfb-treated sample (Figure 3A and Supplementary Figure S5). While the main population of genes showed a slight correlation between the TL value and the CDS length, the other population displayed a very low TL but did not follow such a correlation. These tendencies were even more evident when plotting the difference of TLs of Sfb-treated *versus* control samples (Figure 3B and Supplementary Figure S5). Interestingly, genes whose mRNAs are apparently not subjected to N^6-methyladenosine (m^{6}A) methylation were highly enriched within the 'Sfb hypersensitive genes' category (*p*-value 7.82×10^{-26}; Figure 4 and Supplementary Figure S5). This result is remarkable as it has been recently reported that HCC patients harbour a distinct m^{6}A modification pattern, which contributes to the heterogeneity and diversity of HCC [36,37]. Given these data, we speculate whether inducing global mRNA m^{6}A demethylation could be a promising strategy to make HCC cells more sensitive to Sfb by hindering translation for a broader range of mRNAs. Alternatively, silencing specific m^{6}A methylases could generate the same desired effect. In this regard, target genes of METTL3, which in a complex with METTL14 is the main enzyme

responsible for m^{6}A mRNA methylation [38], are enriched in the set of genes with a high TL in Sfb-treated cells and control conditions, but are not statistical represented in genes with a low TL in Sfb-treated cells (Supplementary Figure S6). However, although the chemotherapeutic potential of drugs affecting m^{6}A-related mechanisms has to be clinically explored in HCC, we must be extremely cautious as our observations are discrepant with the fact that METTL3 has been found to be significantly down-regulated in human Sfb-resistant HCC cells and that knockdown of METTL3 enhances Sfb resistance in HCC by reducing FOX3-mediated autophagy [39].

We finally applied an enrichment analysis using the REACTOME database [40] to identify the cellular context and biological pathways affected by the Sfb-induced reprogramming of translation. We selectively focused on those cellular processes that were translationally up- or down-regulated by the Sfb treatment but down- or up-regulated in the control situation, respectively (Figure 5 and Supplementary Dataset S9). Then, we expanded our analysis by studying those pathways that, being up- or down-regulated in Sfb-treated cells, were not simultaneous up- or down-regulated in the untreated situation, respectively (Figure 6 and Supplementary Dataset S9). We could highlight two global categories including cellular processes containing genes significantly up-regulated upon the Sfb treatment (Figures 5 and 6). First, Sfb seems to selectively induce the translation of processes related to the global metabolism of RNA, more specifically, those related to the maturation and modification of pre-tRNAs and the processing of most abundant pre-mRNAs (capped and intron-containing ones), including their nuclear splicing and further nucleo-cytoplasmic export. The relevance of this finding is unclear; however, we hypothesize that this up-regulation may originate as a positive feedback of
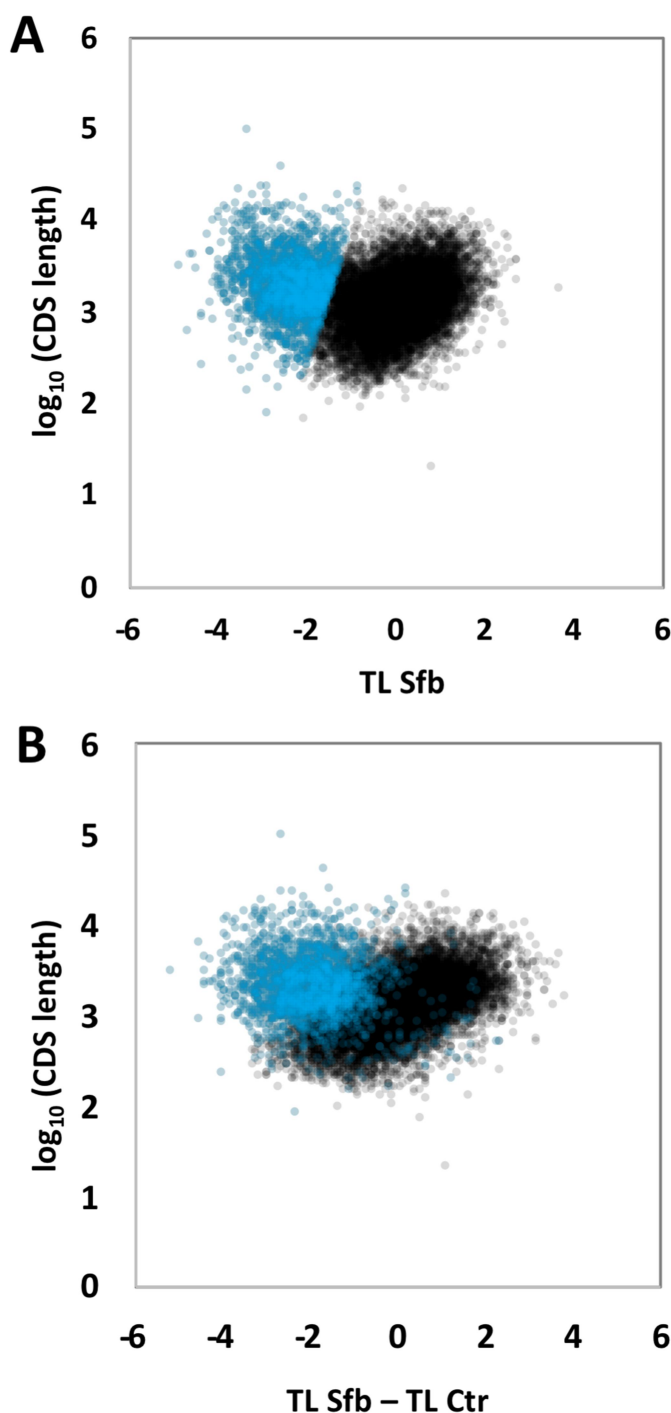
Figure 3. Definition of Sfb hypersensitive genes. A. Scatter plot between the TL in Sfb-treated samples and the $\log_{10}$ of the CDS length. Note that a population of genes with low negative TL, named Sfb hypersensitive genes (in blue), does not follow the general tendency. B. Scatter plot between the difference in TL of the Sfb-treated *versus* the control samples and the $\log_{10}$ of the CDS length. Sfb hypersensitive genes are again highlighted in blue.

mRNA expression to antagonize the Sfb-induced translation repression. Second, Sfb seems to translationally up-regulate components of signal transduction pathways through RAS homolog (RHO) small GTPases, which control many fundamental cellular processes including the actin cytoskeleton formation, gene transcription, cell morphology and movement [41] and have been related to HCC [42]. One of these GTPases is the

so-called MIRO proteins, which are localized in the outer mitochondrial membrane and are involved in mitochondrial biogenesis, maintenance and organization [43]. As these molecular switches are activated by different classes of membrane receptors, including receptors of tyrosine kinases, such as the Sfb-targets VEGFR and PDGFR [44], we interpreted this as the result of a cellular compensatory response to cope with the inhibition exerted by Sfb.

Regarding those cellular processes containing genes translationally down-regulated in Sfb-treated cells, we identified those related to the mitochondrial metabolism, including the electron transport chain and the ATP synthesis, the citric acid cycle, and the mitochondrial translation process (Figure 5). In agreement with this, Sfb has clearly been reported to inhibit respiration and reduce ATP levels [45,46], destroy mitochondrial morphology [47], and down-regulate both the mRNA [13] and protein levels [48] of a large collection of mitochondrial components, including the respiratory chain complex I of the electron transport chain and the mitochondrial ribosome, in different types of cancer cells. Importantly, Sfb resistance is linked to a reprogramming of mitochondrial functions and the activation of mitochondrial translation and biogenesis in HCC cells [49]. Besides targeting genes important for mitochondrial activity, our data revealed that cellular pathways related to the extracellular matrix (ECM) organization (including those involving NCAM1) and the collagen synthesis are also significantly down-regulated in Sfb-treated cells (Figure 6). Collagen is the main component of the ECM, its remodelling influences different aspects of cancer cells, including angiogenesis and migration (e.g. [50,51]), and is valuable as a cancer diagnosis biomarker (e.g. [52]). In consonance with our data, it has been described that Sfb reduces collagen synthesis in mouse and human fibroblasts [53,54] and attenuates liver fibrosis in rats by decreasing collagen accumulation [55,56]. Interestingly, other processes down-regulated by Sfb involve the neuronal system category, particularly those related to K$^+$ channels. These channels regulate a myriad of physiological processes including those related to cell proliferation; K$^+$ channels have also a relevant role in HCC (cell proliferation, migration and invasion) and Sfb resistance (e.g. [57,58]). Reports on drugs targeting distinct K$^+$ channels have been described to enhance the effects of Sfb or reverse Sfb resistance in liver cancer (revised in [57]).

We finally analyse whether the genes belonging to the categories differentially regulated by Sfb were enriched in some of the *cis*-acting mRNA features described above that influences translation. As a result, and as expected, we identified a high number of DAP5-target, CPEB4-target, and ARE- and uORF-containing mRNAs only in the translationally up-regulated processes by Sfb, further revelling the importance of these mRNA elements controlling the translation reprogramming that Sfb induced in HCC cells (Supplementary Figures S7-S12).

In conclusion, although several direct targets of Sfb have been postulated, the exact mechanisms for Sfb-induced cell death and resistance are not fully well understood. In this report, we provide pioneering insights into how Sfb impacts translation in HCC cells. The inhibition of translation by Sfb clearly contributes to its anti-oncogenic efficacy. We have also shown that the cellular stress induced by Sfb also promotes a translation reprogramming in treated cells that seems to
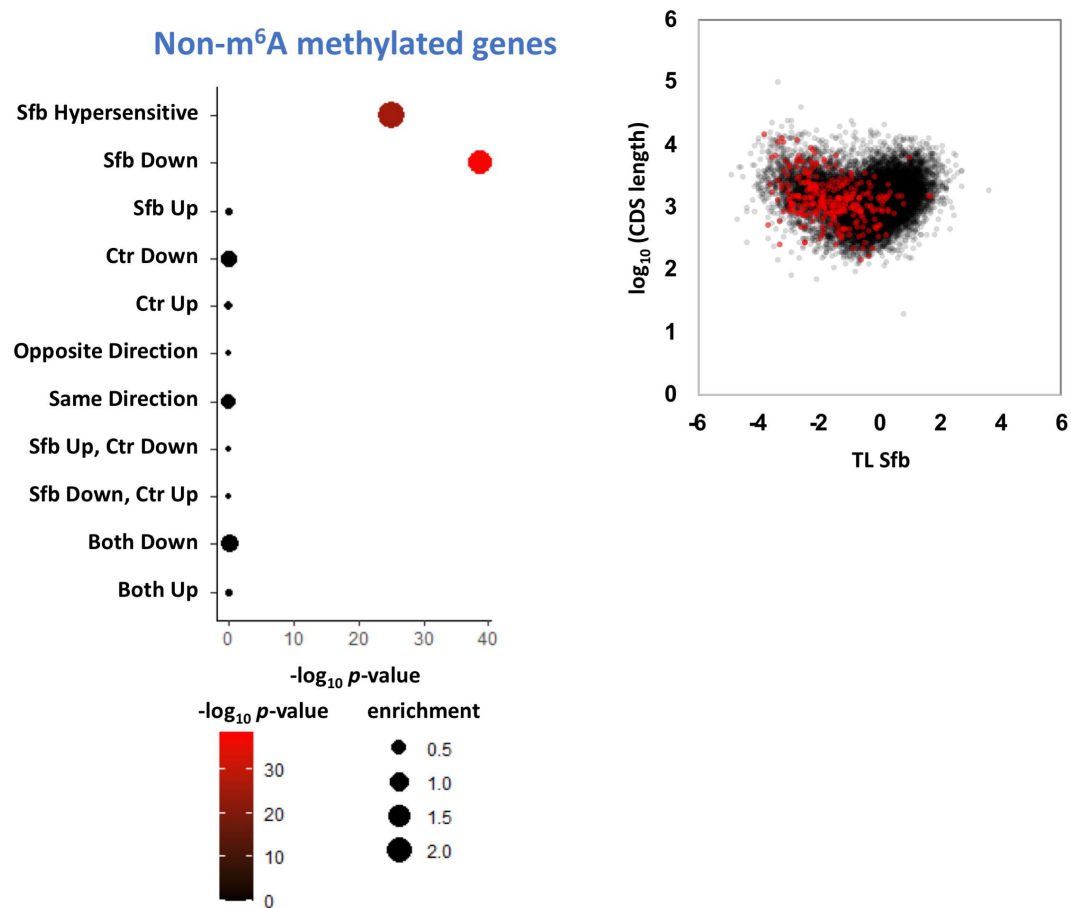
Figure 4. Abundance of non-m⁶A methylated genes in the different categories of our analysis. *Left panel*, bubble plot showing the ORA of non-m⁶A methylated mRNAs within the different gene categories defined in Figure 1B and the group of genes hypersensitive to Sfb. *Right panel*, scatter plot between the TL in Sfb-treated samples and the $\log_{10}$ of the CDS length. Genes coding non-m [6]A methylated mRNAs are highlighted in red.
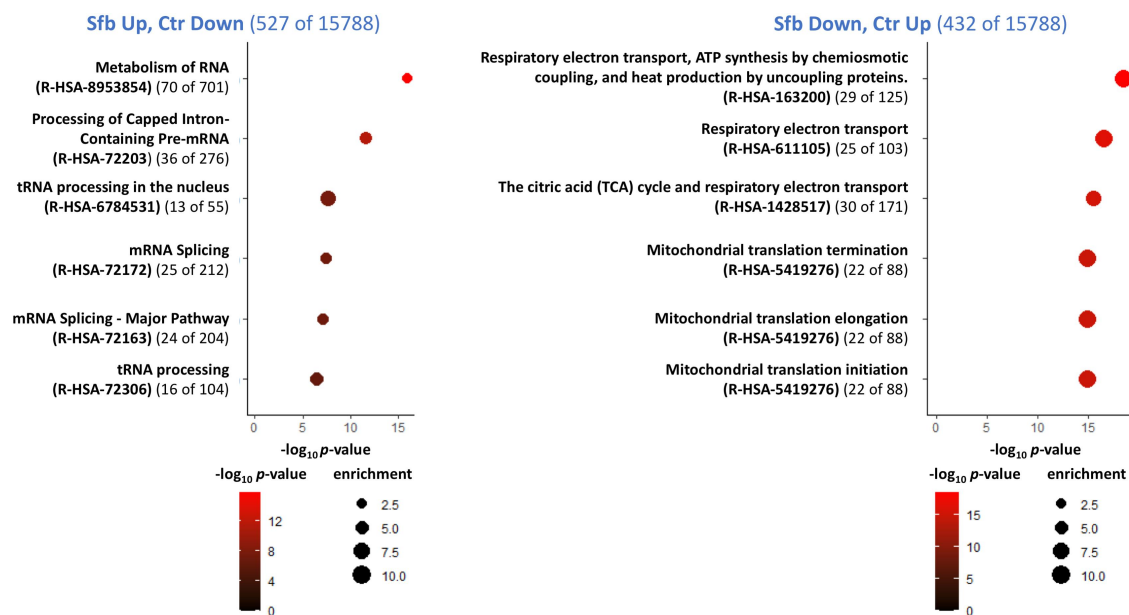

Figure 5. REACTOME functional annotation for genes with an opposite direction identified in our analysis. Bubble plots showing the ORA of the top REACTOME categories in the genes with an opposite direction in Sfb-treated and untreated control samples. *Left panel*, Sfb-up and control-down category. *Right panel*, Sfb-down and control-up category.
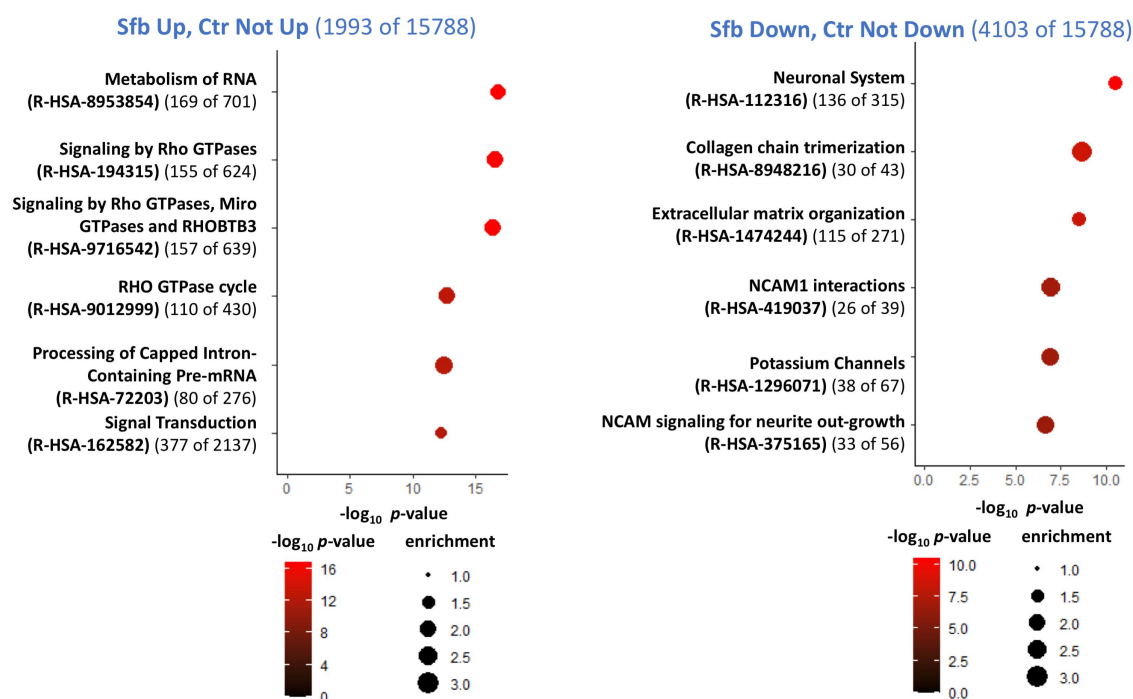
Figure 6. REACTOME functional annotation for specific genes identified in our analysis. Bubble plot showing the ORA of the top REACTOME categories in the genes with an either up-regulated (*left panel*) and down-regulated (*right panel*) translation in the Sfb-treated samples but with a not up-regulated (*left panel*) and down-regulated (*right panel*) translation in control samples, respectively.

operate *via* the involvement of distinct factors (e.g. ATF4, DAP5, ARE-binding proteins) and the recognition of specific *cis*-acting elements in their mRNA targets. This reprogramming involves the repression of global protein synthesis, accompanied by the up-regulation of different cellular pathways. Some of the repressed pathways, such as those related to mitochondrial functions or collagen synthesis, might be related to the anti-tumorigenic activities of Sfb. In contrast, the translational up-regulation of other cellular pathways seems to be a mechanism to counteract the stress effect generated by the drug. Certain basic aspects of RNA metabolism and Rho GTPase signalling are examples of processes that are translationally up-regulated by Sfb but, in parallel, unfortunately, they have been described to be involved in the generation or maintenance of the carcinogenicity of HCC; thus, expecting to contribute to the limited effectiveness Sfb has as a chemotherapeutic drug. We firmly believe that combining Sfb with therapies based on the translational profile of cancer cells, such as the interdiction of the function and/or expression of specific genes in those cellular pathways that are being up-regulated upon a Sfb-treatment could be a future and useful interference approach to enhance the Sfb treatment response and overcome the onset of Sfb resistance. Besides, with further studies in this line, our study could also help to generate tools to predict the response to the Sfb treatment as well as define different cellular processes as biomarkers in the Sfb response.

Acknowledgments

Disclosure statement

Funding

Author contributions statement

L.C. and J.d.l.C. designed the research analyses. L.C. and A.R.-G. performed the research analyses. L.C. and A.R.-G. validated the bioinformatic analyses. L.C., A.R.-G., J.M. and J.d.l.C. analysed the data. L.C. and J.d.l.C. drafted the manuscript. L.C., A.R.-G., J.M. and J.d.l.C. critically revised the manuscript. L.C., A.R.-G., J.M. and J.d.l. C. approved the final version of the manuscript and agreed to be accountable for all aspects of the work.

Data availability statement

The data that support the findings of this study are openly available in the Gene Expression Omnibus (GEO) database https://www.ncbi.nlm. nih.gov/geo/under the accession number GSE282706.

ORCID

Laura Contreras http://orcid.org/0000-0001-8385-4084
Alfonso Rodríguez-Gil http://orcid.org/0000-0003-4430-077X
Jordi Muntané http://orcid.org/0000-0002-6744-1121
Jesús de la Cruz http://orcid.org/0000-0001-5870-659X

References

[1] Vogel A, Meyer T, Sapisochin G, et al. Hepatocellular carcinoma. Lancet. 2022;400(10360):1345–1362. doi: 10.1016/S0140-6736(22)01200-4

[2] Llovet JM, Kelley RK, Villanueva A, et al. Hepatocellular carcinoma. Nat Rev Dis Primers. 2021;7(1):6. doi: 10.1038/s41572-020-00240-3

[3] Reig M, Forner A, Rimola J, et al. BCLC strategy for prognosis prediction and treatment recommendation: the 2022 update. J Hepatol. 2022;76(3):681–693. doi: 10.1016/j.jhep.2021.11.018

[4] Llovet JM, Castet F, Heikenwalder M, et al. Immunotherapies for hepatocellular carcinoma. Nat Rev Clin Oncol. 2022;19(3):151–172. doi: 10.1038/s41571-021-00573-2

[5] Pfister D, Nunez NG, Pinyol R, et al. NASH limits anti-tumour surveillance in immunotherapy-treated HCC. Nature. 2021;592(7854):450–456. doi: 10.1038/s41586-021-03362-0

[6] Llovet JM, Montal R, Sia D, et al. Molecular therapies and precision medicine for hepatocellular carcinoma. Nat Rev Clin Oncol. 2018;15(10):599–616. doi: 10.1038/s41571-018-0073-4

[7] Mou L, Tian X, Zhou B, et al. Improving outcomes of tyrosine kinase inhibitors in hepatocellular carcinoma: new data and ongoing trials. Front Oncol. 2021;11:752725. doi: 10.3389/fonc.2021.752725

[8] da Fonseca LG, Reig M, Bruix J, et al. Tyrosine kinase inhibitors and hepatocellular carcinoma. Clin Liver Dis. 2020;24(4):719–737. doi: 10.1016/j.cld.2020.07.012

[9] Liu L, Cao Y, Chen C, et al. Sorafenib blocks the RAF/MEK/ERK pathway, inhibits tumor angiogenesis, and induces tumor cell apoptosis in hepatocellular carcinoma model PLC/PRF/5. Cancer Res. 2006;66(24):11851–11858. doi: 10.1158/0008-5472.CAN-06-1377

[10] Rahmani M, Davis EM, Crabtree TR, et al. The kinase inhibitor sorafenib induces cell death through a process involving induction of endoplasmic reticulum stress. Mol Cell Biol. 2007;27(15):5499–5513. doi: 10.1128/MCB.01080-06

[11] Rodríguez-Hernández MA, González R, de la Rosa AJ, et al. Molecular characterization of autophagic and apoptotic signaling induced by sorafenib in liver cancer cells. J Cell Physiol. 2018;234(1):692–708. doi: 10.1002/jcp.26855

[12] Sauzay C, Louandre C, Bodeau S, et al. Protein biosynthesis, a target of sorafenib, interferes with the unfolded protein response (UPR) and ferroptosis in hepatocellular carcinoma cells. Oncotarget. 2018;9(9):8400–8414. doi: 10.18632/oncotarget.23843

[13] Contreras L, Rodríguez-Gil A, Muntané J, et al. Broad transcriptomic impact of sorafenib and its relation to the antitumoral properties in liver cancer cells. Cancers (Basel). 2022;14(5):14. doi: 10.3390/cancers14051204

[14] Fucile C, Marenco S, Bazzica M, et al. Measurement of sorafenib plasma concentration by high-performance liquid chromatography in patients with advanced hepatocellular carcinoma: is it useful the application in clinical practice? A pilot study. Med Oncol. 2015;32(1):335. doi: 10.1007/s12032-014-0335-7

[15] Choe J, Lin S, Zhang W, et al. mRNA circularization by METTL3–eIf3h enhances translation and promotes oncogenesis. Nature. 2018;561(7724):556–560. doi: 10.1038/s41586-018-0538-8

[16] Liu S, Zhu A, He C, et al. REPIC: a database for exploring the N(6)-methyladenosine methylome. Genome Biol. 2020;21(1):100. doi: 10.1186/s13059-020-02012-4

[17] Barbieri I, Tzelepis K, Pandolfini L, et al. Promoter-bound METTL3 maintains myeloid leukaemia by m(6)A-dependent translation control. Nature. 2017;552(7683):126–131. doi: 10.1038/nature24678

[18] Bakheet T, Hitti E, Khabar KSA. ARED-Plus: an updated and expanded database of au-rich element-containing mRNAs and pre-mRNAs. Nucleic Acids Res. 2018;46(D1):D218–D220. doi: 10.1093/nar/gkx975

[19] Scholz A, Eggenhofer F, Gelhausen R, et al. uORF-Tools—Workflow for the determination of translation-regulatory upstream open reading frames. PLOS ONE. 2019;14(9):e0222459. doi: 10.1371/journal.pone.0222459

[20] Pérez-Guijarro E, Karras P, Cifdaloz M, et al. Lineage-specific roles of the cytoplasmic polyadenylation factor CPEB4 in the regulation of melanoma drivers. Nat Commun. 2016;7(1):13418. doi: 10.1038/ncomms13418

[21] Zhao J, Li Y, Wang C, et al. Iresbase: a comprehensive database of experimentally validated internal ribosome entry sites. Genomics Proteomics Bioinf. 2020;18(2):129–139. doi: 10.1016/j.gpb.2020.03.001

[22] de la Parra C, Ernlund A, Alard A, et al. A widespread alternate form of cap-dependent mRNA translation initiation. Nat Commun. 2018;9(1):3068. doi: 10.1038/s41467-018-05539-0

[23] Robichaud N, Sonenberg N, Ruggero D, et al. Translational control in cancer. Cold Spring Harb Perspect Biol. 2019;11(7):a032896. doi: 10.1101/cshperspect.a032896

[24] Kovalski JR, Kuzuoglu-Ozturk D, Ruggero D. Protein synthesis control in cancer: selectivity and therapeutic targeting. Embo J. 2022;41(8):e109823. doi: 10.15252/embj.2021109823

[25] Schulze RJ, Schott MB, Casey CA, et al. The cell biology of the hepatocyte: a membrane trafficking machine. J Cell Biol. 2019;218(7):2096–2112. doi: 10.1083/jcb.201903090

[26] Adjibade P, St-Sauveur VG, Quevillon Huberdeau M, et al. Sorafenib, a multikinase inhibitor, induces formation of stress granules in hepatocarcinoma cells. Oncotarget. 2015;6(41):43927–43943. doi: 10.18632/oncotarget.5980

[27] Arzumanian VA, Kiseleva OI, Poverennaya EV. The curious case of the HepG2 cell line: 40 years of expertise. Int J Mol Sci. 2021;22(23):22. doi: 10.3390/ijms222313135

[28] Hetz C, Zhang K, Kaufman RJ. Mechanisms, regulation and functions of the unfolded protein response. Nat Rev Mol Cell Biol. 2020;21(8):421–438. doi: 10.1038/s41580-020-0250-z

[29] Pelletier J, Thomas G, Volarević S. Ribosome biogenesis in cancer: new players and therapeutic avenues. Nat Rev Cancer. 2018;18(1):51–63. doi: 10.1038/nrc.2017.104

[30] Bustelo XR, Dosil M. Ribosome biogenesis and cancer: basic and translational challenges. Curr Opin Genet Dev. 2018;48:22–29. doi: 10.1016/j.gde.2017.10.003

[31] Elhamamsy AR, Metge BJ, Alsheikh HA, et al. Ribosome biogenesis: a central player in cancer metastasis and therapeutic resistance. Cancer Res. 2022;82(13):2344–2353. doi: 10.1158/0008-5472.CAN-21-4087

[32] Gnanasundram SV, Pyndiah S, Daskalogianni C, et al. PI3Kδ activates E2F1 synthesis in response to mRNA translation stress. Nat Commun. 2017;8(1):2103. doi: 10.1038/s41467-017-02282-w

[33] Maillo C, Martín J, Sebastián D, et al. Circadian- and upr-dependent control of CPEB4 mediates a translational response to counteract hepatic steatosis under ER stress. Nat Cell Biol. 2017;19(2):94–105. doi: 10.1038/ncb3461

[34] Weber R, Kleemann L, Hirschberg I, et al. DAP5 enables main ORF translation on mRNAs with structured and uORF-containing 5′ leaders. Nat Commun. 2022;13(1):7510. doi: 10.1038/s41467-022-35019-5

[35] Marash L, Kimchi A. DAP5 and ires-mediated translation during programmed cell death. Cell Death Differ. 2005;12(6):554–562. doi: 10.1038/sj.cdd.4401609

[36] Shen X, Hu B, Xu J, et al. The m6A methylation landscape stratifies hepatocellular carcinoma into 3 subtypes with distinct metabolic characteristics. Cancer Biol Med. 2020;17(4):937–952. doi: 10.20892/j.issn.2095-3941.2020.0402

[37] Yin T, Zhao L, Yao S. Comprehensive characterization of m6A methylation and its impact on prognosis, genome instability, and tumor microenvironment in hepatocellular carcinoma. BMC Med Genomics. 2022;15(1):53. doi: 10.1186/s12920-022-01207-x

[38] He PC, He C. m6A RNA methylation: from mechanisms to therapeutic potential. Embo J. 2021;40(3):e105977. doi: 10.15252/embj.2020105977

[39] Lin Z, Niu Y, Wan A, et al. RNA m6A methylation regulates sorafenib resistance in liver cancer through FOXO3-mediated autophagy. Embo J. 2020;39(12):e103181. doi: 10.15252/embj.2019103181

[40] Jassal B, Matthews L, Viteri G, et al. The reactome pathway knowledgebase. Nucleic Acids Res. 2020;48:D498–D503. doi: 10.1093/nar/gkz1031

[41] Jaffe AB, Hall A. Rho GTPases: biochemistry and biology. Annu Rev Cell Dev Biol. 2005;21(1):247–269. doi: 10.1146/annurev.cellbio.21.020604.150721

[42] Wang T, Rao D, Yu C, et al. RHO GTPase family in hepatocellular carcinoma. Exp Hematol Oncol. 2022;11(1):91. doi: 10.1186/s40164-022-00344-4

[43] Fransson S, Ruusala A, Aspenstrom P. The atypical rho GTPases miro-1 and miro-2 have essential roles in mitochondrial trafficking. Biochem Biophys Res Commun. 2006;344(2):500–510. doi: 10.1016/j.bbrc.2006.03.163

[44] Schiller MR. Coupling receptor tyrosine kinases to rho GTPases—GEFs what's the link. Cell Signal. 2006;18(11):1834–1843. doi: 10.1016/j.cellsig.2006.01.022

[45] Fiume L, Manerba M, Vettraino M, et al. Effect of sorafenib on the energy metabolism of hepatocellular carcinoma cells. Eur J Pharmacol. 2011;670(1):39–43. doi: 10.1016/j.ejphar.2011.08.038

[46] Tesori V, Piscaglia AC, Samengo D, et al. The multikinase inhibitor sorafenib enhances glycolysis and synergizes with glycolysis blockade for cancer cell killing. Sci Rep. 2015;5(1):9149. doi: 10.1038/srep09149

[47] Li Y, Xia J, Shao F, et al. Sorafenib induces mitochondrial dysfunction and exhibits synergistic effect with cysteine depletion by promoting HCC cells ferroptosis. Biochem Biophys Res Commun. 2021;534:877–884. doi: 10.1016/j.bbrc.2020.10.083

[48] Bull VH, Rajalingam K, Thiede B. Sorafenib-induced mitochondrial complex I inactivation and cell death in human neuroblastoma cells. J Proteome Res. 2012;11(3):1609–1620. doi: 10.1021/pr200790e

[49] Pandit SK, Sandrini G, Merulla J, et al. Mitochondrial plasticity promotes resistance to sorafenib and vulnerability to STAT3 inhibition in human hepatocellular carcinoma. Cancers (Basel). 2021;13(23):6029. doi: 10.3390/cancers13236029

[50] Xu S, Xu H, Wang W, et al. The role of collagen in cancer: from bench to bedside. J Transl Med. 2019;17(1):309. doi: 10.1186/s12967-019-2058-1

[51] Roy AM, Iyer R, Chakraborty S. The extracellular matrix in hepatocellular carcinoma: mechanisms and therapeutic vulnerability. Cell Rep Med. 2023;4(9):101170. doi: 10.1016/j.xcrm.2023.101170

[52] Song K, Yu Z, Zu X, et al. Collagen remodeling along cancer progression providing a novel opportunity for cancer diagnosis and treatment. Int J Mol Sci. 2022;23(18):10509. doi: 10.3390/ijms231810509

[53] Wang W, Qu M, Xu L, et al. Sorafenib exerts an anti-keloid activity by antagonizing TGF-β/Smad and MAPK/ERK signaling pathways. J Mol Med (Berl). 2016;94(10):1181–1194. doi: 10.1007/s00109-016-1430-3

[54] Chen YL, Zhang X, Bai J, et al. Sorafenib ameliorates bleomycin-induced pulmonary fibrosis: potential roles in the inhibition of epithelial–mesenchymal transition and fibroblast activation. Cell Death Dis. 2013;4(6):e665. doi: 10.1038/cddis.2013.154

[55] Zhang R, Ma M, Lin XH, et al. Extracellular matrix collagen I promotes the tumor progression of residual hepatocellular carcinoma after heat treatment. BMC Cancer. 2018;18(1):901. doi: 10.1186/s12885-018-4820-9

[56] Wang Y, Gao J, Zhang D, et al. New insights into the anti-fibrotic effects of sorafenib on hepatic stellate cells and liver fibrosis. J Hepatol. 2010;53(1):132–144. doi: 10.1016/j.jhep.2010.02.027

[57] Chen X, Zhang L, He L, et al. Potassium channels as novel molecular targets in hepatocellular carcinoma (review). Oncol Rep. 2023;50(4):185. doi: 10.3892/or.2023.8622

[58] Jiang W, Li G, Li W, et al. Sodium orthovanadate overcomes sorafenib resistance of hepatocellular carcinoma cells by inhibiting Na(+)/K(+)-ATPase activity and hypoxia-inducible pathways. Sci Rep. 2018;8(1):9706. doi: 10.1038/s41598-018-28010-y